Third-harmonic Rayleigh scattering: theory and experiment

Vladislav I. Shcheslavskiy

Department of Physics, University of Wisconsin—Milwaukee, P. O. Box 413, Milwaukee, Wisconsin 53201 and Optoelectronics Research Centre, University of Southampton, Southampton SO17 1BJ, United Kingdom

Solomon M. Saltiel

Faculty of Physics, Sofia University, 5 J. Bourchier Blvd, Sofia, BG-1164, Bulgaria

Alexey Faustov, Georgi I. Petrov, and Vladislav V. Yakovlev

Department of Physics, University of Wisconsin—Milwaukee, P. O. Box 413, Milwaukee, Wisconsin 53201

Received March 21, 2005; revised manuscript received June 9, 2005; accepted June 9, 2005

We present an analytical model for describing optical third-harmonic generation from a sphere that is small compared with the wavelength of light. Analysis of the problem shows that the power of the third harmonic from a sphere that is small compared with the waist size and the confocal parameter of the beam is proportional to the fourth power of a sphere's size. Experiments with different spheres both in index-matching and non-index-matching liquids are performed and confirm theoretical predictions. © 2005 Optical Society of America

OCIS codes: 140.7090, 190.4160, 290.5850, 190.3970, 190.7110.

1. INTRODUCTION

It has long been known that light that is incident on particles that are small compared with the radiation wavelength experiences Rayleigh scattering.[1] Linear light scattering from spherical particles of micrometer size was extensively studied during the past century, both experimentally and theoretically. In 1940 Debye developed light scattering as a method for studying molecular weights, sizes, shapes, and interactions of biological molecules in solutions. Experimental and theoretical developments have helped to advance light scattering as an indispensable and often unique analytical technique with applications in material science, biological imaging, and aerosol sensing.[2,3] One of the main fundamental conclusions of Rayleigh's theory is that the intensity of light scattering is proportional to the sixth power of the particle size for a given wavelength of the incident radiation. This steep dependence on size limits the minimal size of the particle, which can be detected, for example, by using the dark-field microscopy technique. With the advent of ultrashort-pulse lasers and development of nonlinear optics, nonlinear effects in light scattering became increasingly important. Nonlinear optical studies for micrometer and submicrometer particles exploited both second-[4–6] and third-order nonlinear responses.[7–9]

Most of the efforts were concentrated on the possible mechanisms of enhancement of a relatively weak nonlinear optical signal from microparticles. For example, the significant enhancement of the local electric field in the area near the surface of a microscopic particle leads to a tremendous increase of the efficiency of higher-order nonlinear optical processes, such as white-light continuum generation.[10] However, when the particle size becomes smaller than the wavelength of the incident light (Rayleigh particles), no significant local-field enhancement is expected.[11] Thus the absence of these enhanced effects for Rayleigh particles limits the potential of nonlinear optics as a spectroscopic probe for the characterization of microparticles.

A very limited number of experiments have been performed to reveal the exact dependence of the third-harmonic and second-harmonic signals generated from a submicrometer particle on its size.[12,13] Conventional wisdom treats this particle made out of a noncentrosymmetric material as a dipole,[14] with a dipole moment directly proportional to the particle volume, making the total second-harmonic signal proportional to the square of its dipole moment, i.e., scaled in the same way as in linear Rayleigh scattering. Recently, those results were generalized for the case of quadruple and surface dipole contribution to the second-harmonic generation, and it was found that both of those nonlinear polarizabilities scale with the volume of a sphere.[15,16] Thus a scattered second-harmonic power from a particle is proportional to the sixth power of its radius.

Third-harmonic generation (THG) in a plane-wave approximation from metallic particles of arbitrary size has been considered previously.[7,9] Although both theories yielded analytic solutions, the exact analysis was quite complicated, and numerical analysis was required.

In this paper we present a detailed analysis of THG in a focused-beam geometry from dielectric Rayleigh particles, expanding our earlier treatment of the problem.[12,17]

0740-3224/05/112402-7/$15.00

Theory yields the following results:

(i) THG signal from a particle whose radius is smaller than a beam-waist radius, a confocal parameter, and a coherence length, scales as the fourth power of particle radius. This fourth-power dependence puts this nonlinear optical technique in an advantageous position compared with the other scattering methods to detect nanoscopic objects.

(ii) For particles with radii bigger than a beam-waist radius but smaller than a confocal parameter and a coherence length, a third-harmonic signal is proportional to the square of the particle's radius. In this case the dependence of the third-harmonic signal on the radius of particles is a quasi-periodic function with a period of beating of the particle and solution coherence lengths.

We find a good agreement between the results of the theory [fourth-power dependence, (i)] and the experiments. We also demonstrate how this nontrivial effect can be applied to visualize nanosized objects in optically homogeneous (with respect to linear optical properties) media, which could be potentially important for detecting viruses and other nanometer-sized living organisms and organelles in aqueous solution.

The paper is organized as follows. In Section 2 we present some general results on the theory of THG with a focused beam in homogeneous nonlinear media. In Section 3 we apply the results of Section 2 for calculation of third-harmonic power from a single sphere surrounded by a nonlinear media. Experimental results are presented in Section 4. Section 5 is devoted to conclusions.

2. THIRD-HARMONIC GENERATION WITH FOCUSED BEAMS IN HOMOGENEOUS MEDIA

When an incident light wave at frequency ω_1 interacts with a medium, a nonlinear polarization $\mathbf{P}_3$ at frequency $\omega_3=3\omega_1$ is induced:

$$\mathbf{P}_3=\frac{1}{4}\boldsymbol{\chi}^{(3)}\vdots\mathbf{E}_1\mathbf{E}_1\mathbf{E}_1, \tag{1}$$

where $\boldsymbol{\chi}^{(3)}$ is the tensor of the third-order nonlinear optical susceptibility and $\mathbf{E}_1$ is the electric field of the incident wave. To calculate the power of the third harmonic one has to solve the Maxwell's equation for the electric field at frequency ω_3 with the induced polarization given by Eq. (1) as a source.

Assuming an isotropic homogeneous medium, one can derive the following equation in the slow-varying envelope approximation[18]:

$$2i\frac{{n_3}^2\omega_3}{c^2}\frac{\partial E_3}{\partial t}+2ik_3\frac{\partial E_3}{\partial z}+\nabla_T^2E_3=-\frac{4\pi{\omega_3}^2}{c^2}P_3\exp(-i\Delta kz), \tag{2}$$

where $\Delta k=k_3-3k_1$ is the wave-vector mismatch for the fundamental (ω_1) and third-harmonic (ω_3) waves, $E_3(r,z,t)$ and n_3 are the electric field and the refractive index of the medium at the frequency of the third-harmonic wave, respectively. In the typical case of a focused Gaussian beam, the solution of Eq. (2) can be provided in the form of an integral along the direction of light propagation, which turns out to be exactly zero for a homogeneous medium, reflecting the Gouy phase shift experienced by the focused beam.[18] THG under conditions of large group-velocity mismatch is characterized by a nonstationary length L_{nst}, defined by $L_{\mathrm{nst}}=\tau/\alpha$, where τ is the time duration of the fundamental pulses, and the group-velocity mismatch parameter, $\alpha=1/v_3-1/v_1$, where v_3 and v_1 are the group velocities of the third-harmonic and fundamental waves, respectively.[19] The nonstationary length is the distance at which two initially overlapped pulses at different wavelengths become separated by a time equal to τ. In case of polystyrene and pulse durations of 50 fs, for example, $L_{\mathrm{nst}}=600$ μm, which is much bigger then the diameters of the spheres used in our experiments, so we neglect the time derivative in Eq. (2) (quasistatic approximation), and assuming that both the third-harmonic and fundamental beams have Gaussian distribution, we can get an expression for amplitude of the third-harmonic field $A_3(z)$[18]:

$$\frac{\mathrm{d}A_3}{\mathrm{d}z}=i\gamma{A_{10}}^3\frac{\exp(-i\Delta kz)}{(1+i2z/b)^2}, \tag{3}$$

where $\gamma=\{[3\pi^2\chi^{(3)}]/(\lambda_1 n_3)\}$, $b=(2\pi n_1{\omega_0}^2)/\lambda_1$ is a confocal parameter of the focused beam and ω_0 is the spot radius of the beam waist at $1/e$ field radius. Since the spot radii are connected with the relation $\omega_{03}=\omega_{01}/\sqrt{3}$, the two interacting waves have practically the same confocal parameter $b_3\cong b_1=b$. Note that A_3 and A_{10} in Eq. (3) are the amplitudes of the respective harmonics in the center of the beam ($r=0$) at the focal point. The integration of Eq. (3) gives the amplitude of the third harmonic:

$$A_3(z)=i{A_{10}}^3J(\Delta k,z_1,z_2), \tag{4}$$

where $J(\Delta k,z_1,z_2)=\int_{z_1}^{z_2}\gamma(z)\{[\exp(-i\Delta kz)]/[(1+i2z/b)^2]\}dz$. For $z_2-z_1\gg b$ and homogeneous media, $A_3=0$, and consequently $P_3=0$. For $z_2-z_1\ll b$, Eq. (4) can be solved analytically if γ is constant.

3. THIRD-HARMONIC GENERATION WITH FOCUSED BEAMS IN A SINGLE SPHERE

Let us now consider THG in a single sphere (particle) with radius R and nonlinear coupling coefficient γ_s surrounded by an environment with the coefficient γ_m (Fig. 1). Then we have to evaluate total THG signal in the three volumes as shown in Fig. 1:

$$A_3(-\infty,\infty)=i{A_{10}}^3\left[\int_I\gamma_m\frac{\exp(-i\Delta k_mz)}{(1+2iz/b)^2}\mathrm{d}z+\int_{II}\gamma_s\frac{\exp(-i\Delta k_sz)}{(1+2iz/b)^2}\mathrm{d}z+\int_{III}\gamma_m\frac{\exp(-i\Delta k_mz)}{(1+2iz/b)^2}\mathrm{d}z\right]. \tag{5}$$

Considering that the total third-harmonic field at tight focusing conditions is zero in homogeneous medium and

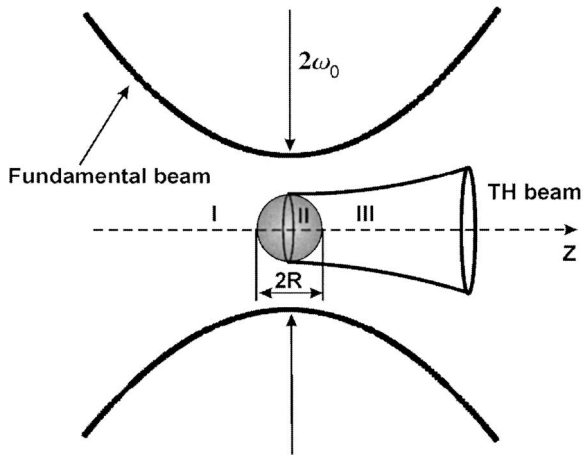

Fig. 1. Schematic diagram illustrating the geometry of third harmonic generation by a small particle in a focused laser beam.

using the same approximation we used for getting the amplitude of third harmonic field in homogeneous medium [Eq. (4)], we get the total third-harmonic amplitude for the case with a sphere in nonlinear media:

$$A_3(-\infty,\infty) = iA_{10}^3 \int_{-L(\rho)/2}^{+L(\rho)/2} (\gamma_s \exp[-i(\Delta k_s + 4/b)z] - \gamma_m \exp[-i(\Delta k_m + 4/b)])\mathrm{d}z, \quad (6)$$

where $L(\rho)=2(R^2-\rho^2)^{1/2}$ if a sphere is in index-matching liquid and $L(\rho)=2R\{1-\sin[\rho^2/(N^2R^2)]\}^{1/2}$ for an arbitrary index of refraction of the solvent; ρ is the distance from the axis z (Fig. 1); $N=n_s/n_m$, n_s and n_m being refractive indexes of a sphere and a medium at fundamental frequency, respectively. We should note that Eq. (6) is obtained with assumptions that radius of a sphere is much less than a confocal parameter and is located in focus of the laser beam. Then the intensity of the third harmonic in the center of the beam is

$$I_3 = \frac{cn_3}{2\pi}\left(\frac{8\pi}{cn_1}I_1\right)^3\left[\frac{\gamma_s}{\tilde{\Delta}k_s}\sin(\tilde{\Delta}k_s L/2) - \frac{\gamma_m}{\tilde{\Delta}k_m}\sin^2(\tilde{\Delta}k_m L/2)\right], \quad (7)$$

where we have introduced the effective mismatches $\tilde{\Delta}k_s = \Delta k_s + 4/b$ and $\tilde{\Delta}k_m = \Delta k_m + 4/b$. Finally, we get an expression for power of the third harmonic by integrating the intensity over beam area:

$$P_3 = \frac{512\pi^3 n_3}{c^2 n_1^3} I_1^3 \int_0^R \rho g^2(\rho)\left[\frac{\gamma_s}{\tilde{\Delta}k_s}\sin(\tilde{\Delta}k_s L/2) - \frac{\gamma_m}{\tilde{\Delta}k_m}\sin^2(\tilde{\Delta}k_m L/2)\right]\mathrm{d}\rho, \quad (8)$$

where $g(\rho)=\exp[-(3\rho^2/\omega_0^2)]$. In the general case the integral in Eq. (8) must be performed numerically.

An analytical solution is possible in the limiting cases when $R \ll \omega_0$ and $R \gg \omega_0$:

(a) In case of $R \ll \omega_0$ Eq. (8) can be integrated analytically for an index-matching surrounding environment (i.e., $n_{\mathrm{sphere}}=n_{\mathrm{medium}}$), which, after integration over the area, perpendicular to the direction of light propagation, gives the following simple formula to calculate the third-harmonic power P_3 generated from a microsphere:

$$P_3 = C(T_s + T_m + T_3),$$

$$\text{where } C = \frac{4096 n_3}{c^2 n_1^3 \omega_0^6} P_1^3, \quad (9)$$

where P_1 is the power of the incident fundamental beam and

$$T_{s,m} = \left(\frac{\gamma_s}{2\tilde{\Delta}k_{s,m}^2}\right)^2 [R^2\tilde{\Delta}k_{s,m}^2 - R\tilde{\Delta}k_{s,m}\sin(2R\tilde{\Delta}k_{s,m}) + \sin^2(R\tilde{\Delta}k_{s,m})],$$

$$T_3 = \frac{\gamma_m\gamma_s}{\tilde{\Delta}k_s\tilde{\Delta}k_m\Delta k_p^2\Delta k_o^2}[R\Delta k_o^2\Delta k_p\sin(R\Delta k_p) - \Delta k_p^2\cos(R\Delta k_o) - R\Delta k_o\Delta k_p^2\sin(R\Delta k_o) + \Delta k_o^2\cos(R\Delta k_p) + 4\tilde{\Delta}k_m\tilde{\Delta}k_s],$$

where $\Delta k_p = \tilde{\Delta}k_s + \tilde{\Delta}k_m$ and $\Delta k_o = \tilde{\Delta}k_s - \tilde{\Delta}k_m$.

For spheres with small radius $R\tilde{\Delta}k_s \ll 1$ and $R\tilde{\Delta}k_m \ll 1$ we get the power of the third harmonic:

$$P_3 = 1024\frac{n_3}{c^2 n_1^3 \omega_0^6}(\gamma_s - \gamma_m)^2 R^4 P_1^3. \quad (10)$$

Clearly, the third-harmonic power depends on the fourth power of the sphere's radius. It can be understood from a set of simple arguments that the third-harmonic power generated by a focused laser beam is proportional to the square of the medium thickness (i.e., $\propto R^2$). In addition, the third-harmonic signal is proportional to the cross section of the sphere (i.e., again $\propto R^2$), since the area of the laser beam, which does not contain sphere's material, does not contribute to the third-harmonic signal.

It is interesting to note that in the case of neutral metallic clusters irradiated by strong ($I \approx 10^{16}$ W/cm^2) linearly polarized subpicosecond pulses, when the third harmonic is resonant with plasmon frequency, theory predicts fourth-power dependence of a third-harmonic signal on the particle's size.[20] However, the origin of fourth-power dependence is different. THG in this case can be seen as being induced by the surface charges of the sphere. Therefore the induced dipole moment is proportional to the area of the sphere rather than to its volume. This leads to a third-harmonic signal varying as the fourth power of the sphere's radius.

(b) In the case of $R \gg \omega_0$ the length L does not depend on ρ and the integration limit in Eq. (8) for ρ can be set to ∞. Then the power of third harmonic is

$$P_3 \propto {I_1}^3 \left(\frac{\pi}{6}{\omega_0}^2\right)\left[\frac{\gamma_s}{\tilde{\Delta}k_s}\sin(\tilde{\Delta}k_s R) - \frac{\gamma_m}{\tilde{\Delta}k_m}\sin(\tilde{\Delta}k_m R)\right]. \tag{11}$$

It can be easily seen that third-harmonic power scales as the second power of the sphere's radius. The results of theoretical calculations [Eqs. (9) and (11)] are presented in Figs. 2 and 3, respectively. From Fig. 2 (inset) we can see that for spheres with radiuses up to 0.8 μm the third-harmonic signal scales as a fourth power of the sphere's diameter.

4. EXPERIMENTAL RESULTS

Owing to the lack of the appropriate laser source to fulfill the requirement $\omega_0 \ll R < \lambda$ we performed all experiments only for the conditions under which $R \ll \omega_0$ and $R < \lambda$ simultaneously.

To check our theoretical conclusions experimentally, we chose to study suspensions of fused-silica (FS) nanoparticles (Bangs Laboratories, Inc.). Our choice was determined by the well-known optical properties of silica. To obtain an index-matching liquid with $n_L = n_{FS} = 1.44$, we mixed benzyl alcohol ($n_{BA} = 1.54$) with methanol ($n_M = 1.32$) in appropriate proportions. We prepared suspensions with silica particles ranging in size from 200 nm to 1 μm. Since there was no scattering owing to inhomogeneities of the medium, the suspensions were transparent.

Suspensions with several different concentrations were prepared for each particle size. The concentration of the particles was kept low enough to avoid agglomeration and to minimize the possibility of having more than one particle in the focal volume. We used the output of a femtosecond Cr:forsterite oscillator (center wavelength $\lambda = 1.25$ μm, pulse duration $\tau = 40$ fs, output average power $P = 300$ mW) as an excitation source.[21] The laser beam was focused with a high-numerical-aperture (NA = 0.4) aspheric lens into a flow-through fused silica cell. The total focal volume was less than 10^{-10} cm^{-3}. The highest concentration of nanoparticles in the suspensions was less

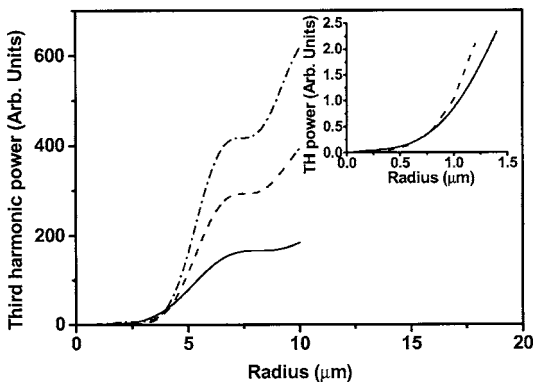

Fig. 2. Results of theoretical calculations of THG in microspheres in an index-matching liquid. Third-harmonic power is in arbitrary units. $R \ll \omega_0$, $b = 32$ μm. Solid curve, $\chi_s^{(3)}/\chi_m^{(3)} = 0.5$; dashed curve, $\chi_s^{(3)}/\chi_m^{(3)} = 2$; dotted–dashed curve, $\chi_s^{(3)}/\chi_m^{(3)} = 3$. Inset, comparison of fourth-power dependence (dashed curve) and plot of analytical Eq. (12) for particles with small diameters.

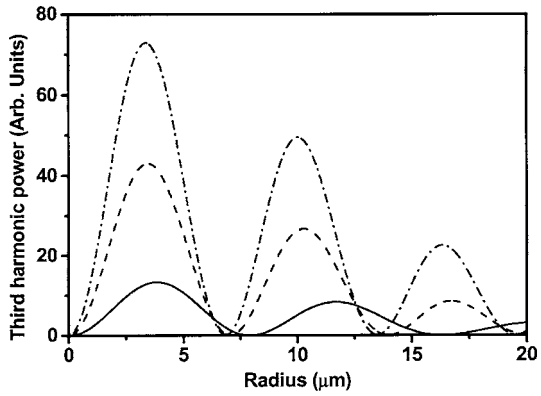

Fig. 3. Theoretical calculations of THG in microspheres in an index-matching liquid. Third-harmonic power is in arbitrary units. $R \gg \omega_0$, $b = 32$ μm. Solid curve, $\chi_s^{(3)}/\chi_m^{(3)} = 0.5$; dashed curve, $\chi_s^{(3)}/\chi_m^{(3)} = 2$; dotted–dashed curve, $\chi_s^{(3)}/\chi_m^{(3)} = 3$.

than 10^8 cm^{-3}, i.e., the probability of finding simultaneously more than one particle in the focal volume is 2 orders of magnitude smaller than the probability of finding just one particle. The presence of the index-matching liquid removes the possibility of particle trapping in the focal spot of the laser beam and facilitates the comparison of experimental results with theory.

The laser beam was focused approximately 200 μm below the surface of the cell wall. At this distance from the surface, we did not observe any contribution to the measured third-harmonic signal from the particles by the third harmonic generated owing to the broken symmetry at the liquid–glass interface, which can be quite strong. We also ensured that the third-harmonic signal essentially disappears when pure index-matching liquid with no suspended particles is placed inside the flow-through cell. (In fact, there was a small nonvanishing background, which scaled as the third power of the incident light intensity. We attribute this background to the second-order Hyper–Rayleigh scattering.) The generated third-harmonic signal was collected in transmission using another high-numerical-aperture (NA = 0.5) aspheric lens and redirected into a multichannel spectrometer with liquid-nitrogen-cooled CCD camera detection. No attempts were made to measure the exact angular dependence of the generated third-harmonic signal. However, we did check that most of the generated third-harmonic radiation in the presence of microspheres was in the forward-propagating direction. The spectrum of the measured third-harmonic signal was identical to the spectrum of the theoretically predicted third harmonic derived from the spectrum of the incident femtosecond pulse. We confirmed the third-power dependence of the generated third harmonic on the incident light intensity by varying the power of the incoming laser beam. For each concentration, we normalized the power of the third-harmonic signal generated inside the solution to the one generated at the air–glass interface. This procedure allows us to take into account any possible effect of absorption and scattering (if any) of either fundamental or the third-harmonic radiation in the suspension, since both waves are traveling through liquid layers with essentially the same thickness.[22] A typical dependence of the spec-

trally and temporally integrated third-harmonic signal as a function of particle concentration in the suspension is shown in Fig. 4. The linear dependence of the third-harmonic signal on concentration proves the earlier assumption about the low probability of finding a particle in the focal volume. In fact, if we raise the concentration above the one for which we should expect a high-enough probability of finding more than one particle in the focal volume, this dependence becomes strongly nonlinear and requires much more sophisticated tools for analysis. We used these raw data to calculate the third-harmonic signal generated by a single particle by normalizing the measured signal by the concentration at which it was measured (i.e., taking the slope of the curve in Fig. 4). The resulting values are plotted in Fig. 5 as a function of microsphere size. Microspheres provided to us are quoted to have a 10% size distribution, which was independently confirmed by scanning electron microscopy of the residue from the dried suspension and is reflected by the horizontal bars in Fig. 5. The fourth-power dependence is shown to provide a guide to the eye and is in very good agreement with our experimental data. To provide a better proof for the fourth-power dependence, one must use a larger dynamic range of microsphere diameters. It is also important that when no index-matching liquid is used, the absolute power of the generated third-harmonic signal changes significantly, since the discontinuity of the refractive index also contributes (and quite significantly) to the generated signal. However, the overall fourth-power dependence of this signal on the microsphere diameter remains the same. In a separate experiment, we used polystyrene microspheres, which were available to us in sizes from 50 nm to 1 μm. We did not use any index-matching liquid in this series of experiments. To exclude any possible effect of particle trapping by the intense laser beam, we properly attenuated the incident laser light to avoid any effect on the particle motion through the focal volume. We followed the above-described procedure to measure the signal dependence on the concentration and to calculate the third-harmonic signal from a single microsphere. The power of the third-harmonic signal generated by a single microsphere as a function of the microsphere diameter is shown in Fig. 6 and once again confirms the fourth-power dependence.

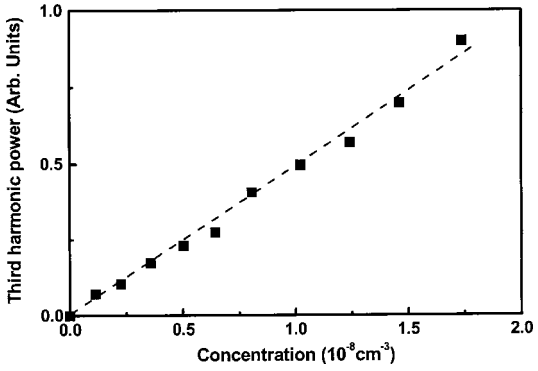

Fig. 4. Power of the third harmonic generated from the solution of 0.750 μm diameter fused-silica particles in the index-matching solution as a function of particle concentration. The dashed line provides a linear fit, used to calculate the effective power of the third harmonic generated by a single particle.

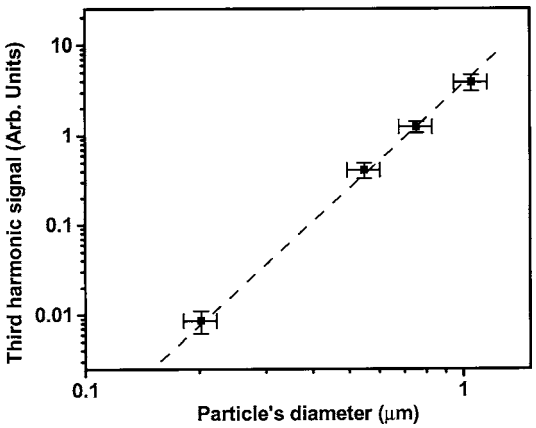

Fig. 5. Third-harmonic intensity generated by a single particle in the index-matching liquid as a function of particle diameter. The dashed line shows the fourth-power dependence.

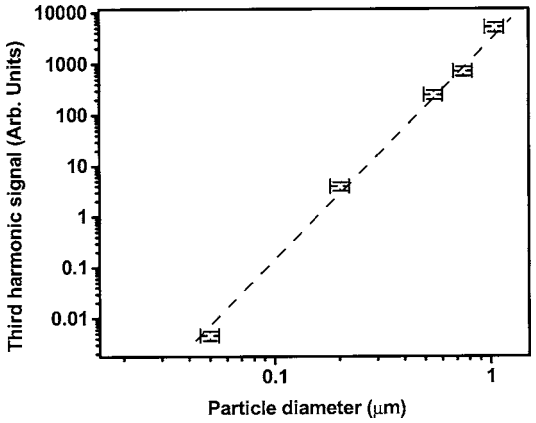

Fig. 6. Power of the third harmonic generated by a single particle in the non-index-matching solution as a function of particle's diameter. The dashed line shows the fourth-power dependence.

It is important to note that from the two measurements of third-harmonic—one generated at the interface glass solution and another one from the bulk of the solution—it is possible to determine both the size of the spheres and their third-order nonlinear susceptibility. Indeed, the nonlinear susceptibility of the solution containing the microspheres $[\chi^{(3)}_{\text{eff}}]$ is determined by the susceptibility of the solution without microspheres $[\chi^{(3)}_m]$ and the susceptibility of the microsphere itself $[\chi^{(3)}_s]$[23]:

$$\chi^{(3)}_{\text{eff}} = \chi^{(3)}_m + p\chi^{(3)}_s, \tag{12}$$

where p is the volume fraction of the spheres in the solution. We can determine $\chi^{(3)}_s$ of the microspheres (surface measurements) using the expression for third-harmonic power obtained in Eq. (3) (Ref. 18) and Eq. (12). Then the size of the spheres can be obtained from Eq. (10), provided the generated third-harmonic power is known from the experiment.

5. CONCLUSIONS

The strength of the third-harmonic Rayleigh scattering is of considerable importance from an experimental viewpoint. Since the third-harmonic signal from a particle is

weak, we examine power of the third-harmonic Rayleigh scattering and apply this result to infer a typical range of experimentally accessible particle sizes. With the current level of experimental techniques 1 nW power can easily be measured. Assuming pulse energy and duration are 15 nJ and 50 fs, respectively, and that the beam is focused in a spot size of 4 μm, we estimate that particles with radii down to 10 nm can be easily detected.

Indeed, we note that the third-harmonic signal generated from the smallest-size ($d=50$ nm) particles is rather strong and is clearly detectable even for a particle density as low as 10^7 cm^{-3}. Our preliminary results show that if a single polystyrene nanoparticle is placed in the focal volume and is trapped there using a tightly focused laser beam the generated third-harmonic signal can be routinely measured by a photomultiplier tube with the number of photocounts being about 10^5 s^{-1}. Our current setup can be also used to count the number of particles passing through a localized focal volume of the laser beam. A typical temporal trace shows particles passing through the focus with a resolution better than 100 ms (Fig. 7). This rather-high number of third-harmonic photons can be further increased by choosing a proper material of the nanospheres. If those nanospheres were made out of nanostructured ZnO,[24] which has a third-order nonlinearity 3 orders of magnitude higher than that of polystyrene, then the total third-harmonic signal would be 6 orders of magnitude stronger, leading to a bright nanoscopic source of third harmonic light ($\lambda=417$ nm). This provides a completely new approach to nanoscopic optical imaging, which was originally suggested to utilize the second-harmonic generation technique[25] but was put aside because of impractically low signal levels for the reasons described at the beginning of this manuscript.

Another potential application of our results deals with the measurement of characteristics of single cells suspended in a flowing saline stream (flow cytometry). Normally, the total amount of forward-scattered light is closely correlated with cell size, and the amount of side scattered light can indicate nuclear shape and cellular granularity. However, such further properties of the cell as intracellular constituents can be accurately quantitated if the cellular marker of interest can be labeled with fluorescence dye. In the case of THG applied for flow cytometry no labeling is required, since all information about cellular structure and properties is supplied by the molecules of interest.

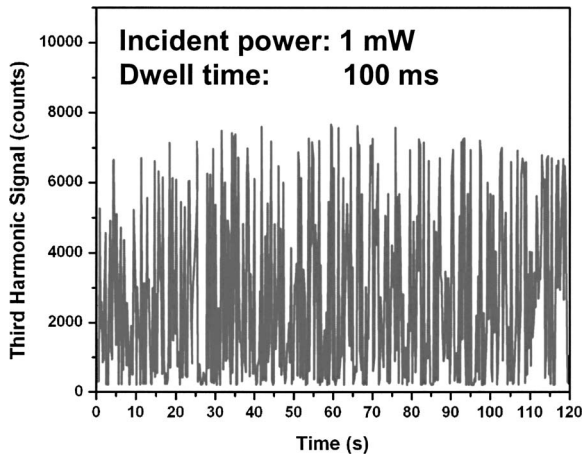

Fig. 7. Time-dependent third-harmonic signal from the bulk of the flowing solution; each spike corresponds to a 200 nm diameter particle passing through a focal volume of a laser beam.

Finally, the results of this work can be applied for material diagnostics. If a small inhomogeneity that is typically different from the rest of the material either in linear or nonlinear optical properties is present inside the material it will manifest itself in the third-harmonic signal. With our present system, assuming that the fourth-power dependence holds on for the smaller-size inhomogeneities, it should be possible to detect nanodefects inside the material as small as 10 nm. Clearly, there are many untapped possibilities for nanoparticle detection based on the discovered anomalous dependence of the generated third-harmonic signal on particle size.

In summary, we have demonstrated both experimentally and theoretically that the third-harmonic power generated by a small particle ($R \ll \omega_0, b, l_{\mathrm{coh}}$) is scaled as the fourth power of the particle's radii and can be strong enough to provide bright nanoscopic sources of light. For spheres with radii bigger than beam waist ω_0 but smaller than confocal parameter b ($R \gg \omega_0, R \ll b$) third-harmonic signal is proportional to R^2 when $R/l_{\mathrm{coh}} \ll 1$. In this case, the dependence of third-harmonic energy on R is a quasi-periodic function with a period determined by the coherence lengths of the material of the sphere and the solvent.

ACKNOWLEDGMENTS

We gratefully acknowledge the partial support for this research by the National Science Foundation (Grant 9984225 and Grant 0210879-NER) and National Institutes of Health (Grant R21RR16282). S. Saltiel and G. I. Petrov acknowledge the North Atlantic Treaty Organization's support (Grant CLG 979419).

REFERENCES

1. J. W. Strut, "On the light from the sky, its polarization and color," Philos. Mag. **41**, 107–120 (1871).
2. C. F. Bohren and D. Huffman, *Absorption and Scattering of Light by Small Particles* (Wiley, 1998).
3. P. W. Barber and R. K. Chang, *Optical Effects Associated with Small Particles* (World Scientific, 1988).
4. X. M. Hua and J. I. Gersten, "Theory of second harmonic generation by small metal spheres," Phys. Rev. B **33**, 3756–3764 (1986).
5. H. Wang, E. Yang, E. Borguet, and K. Eisenthal, "Second harmonic generation from the surface of centrosymmetric particles in bulk solution," Chem. Phys. Lett. **259**, 15–20 (1996).
6. J. I. Dadap, J. Shan, K. B. Eisenthal, and T. F. Heinz, "Second-harmonic Rayleigh scattering from a centrosymmetric material," Phys. Rev. Lett. **83**, 4045–4048 (1999).
7. J. P. Dewitz, W. Hubner, and K. H. Bennemann, "Theory of nonlinear Mie-scattering from spherical metal clusters," Z. Phys. D **37**, 75–84 (1996).
8. J. Kasparian, B. Kramer, J. Dewitz, S. Vajda, P. Rairoux, B. Vezin, V. Boutou, T. Leisner, W. Hubner, J. Wolf, L. Woste, and K. Bennemann, "Angular dependences of third harmonic generation from microdroplets," Phys. Rev. Lett. **78**, 2952–2955 (1997).
9. D. Caroll and X. H. Zheng, "Spatial and angular

distributions of third harmonic generation from metal surfaces," Eur. Phys. J. D **5**, 135–144 (1999).
10. C. Favre, V. Boutou, S. Hill, W. Zimmer, M. Krenz, H. Lambrecht, J. Yu, R. Chang, L. Woeste, and J. Wolf, "White-light nanosource with directional emission," Phys. Rev. Lett. **89**, 035002 (2002).
11. Z. Wang, B. Luk'yanchuk, M. Hong, Y. Lin, and T. Chong, "Energy flow around a small particle investigated by classical Mie theory," Phys. Rev. B **70**, 035418 (2004).
12. V. Shcheslavskiy, G. Petrov, S. Saltiel, and V. Yakovlev, "Quantitative characterization of aqueous solutions probed by the third-harmonic generation microscopy," J. Struct. Biol. **147**, 42–49 (2004).
13. M. Lippitz, M. A. van Dijk, and M. Orrit, "Third-harmonic generation from single gold nanoparticles," Nano Lett. **5**, 799–802 (2005).
14. L. Malmqvist and H. Hertz, "Second harmonic generation in optically trapped nonlinear particles with pulsed lasers," Appl. Opt. **34**, 3392–3397 (1995).
15. V. L. Brudny, B. S. Mendoza, and W. L. Mochan, "Second-harmonic generation from spherical particles," Phys. Rev. B **62**, 11152–11162 (2000).
16. J. I. Dadap, J. Shan, and T. F. Heinz, "Theory of optical second-harmonic generation from a sphere of centrosymmetric material: small-particle limit," J. Opt. Soc. Am. B **21**, 1328–1347 (2004).
17. V. I. Shcheslavskiy, G. I. Petrov, V. V. Yakovlev, S. M. Saltiel, B. S. Luk'yanchuk, Z. S. Nickolov, and J. D. Miller, "Third-harmonic generation from Rayleigh particles," Phys. Rev. Lett., submitted for publication.
18. J. F. Reintjes, *Nonlinear Optical Parametric Processes in Liquids and Gases* (Academic, 1984).
19. S. M. Saltiel, K. Koynov, B. Agate, and W. Sibbett, "Second-harmonic generation with focused beams under conditions of large group-velocity mismatch," J. Opt. Soc. Am. B **21**, 591–598 (2004).
20. S. V. Fomichev, S. V. Popruzhenko, D. F. Zaretsky, and W. Becker, "Laser-induced nonlinear excitation of collective electron motion in a cluster," J. Phys. B **36**, 3817–3834 (2003).
21. V. Shcheslavskiy, V. Yakovlev, and A. Ivanov, "High-energy self-starting Cr^{4+}:Mg_2SiO_4 oscillator operating at low repetition rate," Opt. Lett. **26**, 1999–2001 (2001).
22. V. Shcheslavskiy, G. Petrov, and V. V. Yakovlev, "Nonlinear susceptibility measurements of solutions using third-harmonic generation on the interface," Appl. Phys. Lett. **82**, 3982–3984 (2003).
23. D. Stroud and V. Wood, "Decoupling approximation for the nonlinear-optical response of composite media," J. Opt. Soc. Am. B **6**, 778–786 (1989).
24. G. I. Petrov, V. I. Shcheslavskiy, V. V. Yakovlev, I. Ozerov, E. Chelnokov, and W. Marine, "Efficient third-harmonic generation in a thin nanocrystalline film of ZnO," Appl. Phys. Lett. **83**, 3993–3995 (2003).
25. L. Malmqvist and H. M. Hertz, "Two-color trapped particle optical microscopy," Opt. Lett. **19**, 853–855 (1994).